



Study of the Influence of Laser Welding Parameters on the Weld Quality and Microstructure of S355JR Structural Steel

V. F. C. Sousa¹, F. J. G. Silva^{1,2}(✉), R. D. S. G. Campilho¹, A. G. Pinto¹, and J. S. Fecheira¹

¹ ISEP—School of Engineering, Polytechnic of Porto, Porto, Portugal
{vcris, fgs, app, jsf}@isep.ipp.pt

² INEGI—Instituto de Ciência e Inovação em Engenharia Mecânica e Engenharia Industrial, Porto, Portugal

Abstract. Welding is employed greatly in the construction industry, with processes such as SMAW being the most used for welding structural steels. However, processes such as laser welding exhibit quite some advantages when compared to the conventionally used welding processes, offering the possibility to obtain welded joints in a faster manner, without the need for filler metals, even causing an improvement in mechanical properties, in some cases. There are, however, some limitations with the laser welding of structural steels, especially lack of penetration, which can cause welding defects, such as porosities and voids. In the present work, S355JR steel profiles with 8 mm thickness are produced by laser welding. This weld was analyzed, identifying possible defects, assessing weld quality and grain size, by performing SEM and EBSD analyses. The welding process was then adapted and used to produce thick S355JR steels, with 25 mm thickness. As for the thinner profiles, the weld quality was assessed and characterized, identifying possible defects and the feasibility of employing the laser welding process on the joining of thick structural steel plates.

Keywords: Laser welding · Structural steel · Microstructure · EBSD

1 Introduction

Although additive manufacturing has received particular attention in research over the last two decades, the process is still not able to respond to many of the current market needs, particularly at a structural level. Thus, welding continues to be an extremely used process in terms of relatively thin or large parts. Effectively, the emergence of new materials and the traditional problems presented by other ones, has led to the fact that welding has remained a top issue within Mechanical Engineering [1, 2]. Simulation studies have been another topic of great interest in the field of welding, proving to be a valuable tool for the prediction of microstructures and defect generation, promoting a significant saving of time and resources [3]. Laser welding initially had a high dynamic in the presentation of studies about the process but, due to performance limitations

and robotic applications, it stagnated in terms of development for some time. With the emergence of new laser technologies, namely fiber lasers and disc lasers [4], and the possibility of generating the laser beam at the end of the robot without needing it to support the entire weight of the beam generation system [5], gave way to a new wave of investigations on the process, applying it to the most diverse metal alloys [6, 7], and even polymers [8]. The possibility of robotization gave rise to larger structural parts that could be welded more expeditiously, so laser welding started to be investigated when applied to structural materials, both in similar and dissimilar joints [9, 10].

Grünenwald et al. [11] studied the influence of the oscillation of a fiber laser beam with 10 kW in the welding of structural steel plates with 15 mm of thickness, verifying that the oscillation frequency was around 200 Hz, low welding speed and high beam power was the set of conditions that contributed to obtaining weld seams with the most appropriate geometry for the studied joint. Üstündağ et al. [12] investigated the welding of 25 mm thick S355J2 steel plates through a single pass using a laser beam. Given the thickness of the plates and full penetration is intended, there is usually drop formation. To avoid this problem, the authors successfully used an innovative concept of melt pool support based on generating Lorentz forces. Optimal results were achieved in terms of impact strength and tensile strength using welding speed of 0.9 m/min and 19 kW Laser power. Sokolov et al. [13] also studied penetration and hardness in the same type of structural steel (S355) with 20 and 25 mm thickness, when welded with fiber laser. It was possible to verify that the surface of the welded zone showed a hardness about 2.5 times greater (450–500 HV) than the surface hardness of the base material. For 20 mm thick steel, speed between 1.8 and 2.4 m/min was applied, using power between 15 and 20 kW. When 25 mm thick sheet of the same steel was used, the same speed range was maintained, but the power needed to be increased to the range between 20 and 30 kW. Focal lengths ranged from 7.5 mm for the thinnest plate, and 12.5–15 mm for the thickest one. It was also found that increasing the welding speed decreases the width of the heat affected zone and increases the hardness of the weld bead.

Part of the same team [14] also studied the welding of 40 mm thick SM400A structural steel, using a disc laser with a power of 16 kW at a speed of 1 m/min. Using a polished edge surface ($R_a = 0.4 \mu\text{m}$), a gap of 0.2 mm and a focal length of 20 mm, it was possible to achieve a penetration of 30 mm in the joint. Increasing the roughness edge surface to $6.3 \mu\text{m}$ and gap to 0.3 mm, a penetration of 38 mm was achieved, however not attaining the desired level of quality (lack of fill). Part of the same group of researchers [15] analyzed the influence of the surface roughness of the contact area of the joint to be welded on the penetration obtained by the weld bead, using as base material the same S355 steel and another St3 steel, both with 20 mm of thickness and in butt joint configuration. A fiber laser with power between 10 and 15 kW was used. The maximum penetration was obtained for a roughness of $6.3 \mu\text{m}$ (tested range: 1.6–8.0 μm), verifying from then on, a degradation in the quality of the welded joint.

Laser welding of structural steels is not heavily researched. There are quite some beneficial possibilities in applying this process to the production of structural steel profiles, by reducing the welding time and the overall profile's weight, as these are usually obtained by welded processes that use filler metal. As such, the conducted work aims to provide more knowledge about the laser welding of these thick structural steel profiles,

by showing the welding of two types of thick structural steel profiles and characterizing these welds.

2 Materials and Methods

The following subsections will contain information regarding the materials that were used for the conduction of the presented work, as well as the various employed methods for the welded profile production and analysis.

2.1 Materials

Regarding the materials used, S355JR was the chosen profile material. This steel has the following chemical composition (%wt): 0.24% C, 0.55% Si, 1.60% Mn, 0.035% P, 0.035% S, 0.012% N and 0.55% Cu. Regarding mechanical properties, the steel has an average hardness value of 165 HV5, a yield strength of 355 MPa and a tensile strength of 550 MPa.

For the welding of the thinner profile type, 8 mm thick plates were used, regarding the welding of the thicker profile type, one plate with 25 mm thickness was welded to a 30 mm thick plate, with the 25 mm plate being obtained being cold and hot rolled, while the 30 mm plate was only hot rolled. Due to this fact, these thicker plates differ in terms of microstructure, however, their mechanical properties and composition did not present significant differences. A total of 6 profiles were welded, 3 for each type.

2.2 Methods

In this subsection all the methods for the production and analysis of the welded profiles are going to be presented, starting with the presentation of the chosen process parameters to produce both profile types.

Regarding the laser equipment that was used for welding, a 10 kW maximum power fibre laser was chosen, using as shielding gas Ar⁺ with a flow rate of 20 l/min. To produce the 8 mm thick profiles, the weld was achieved by using 1 laser beam having 4 kW of power, at a welding speed of 1 m/min and an entry angle of 10°. As for the thicker profile, two plates, one having 25 mm thickness and the other 30 mm, were joined by 2 laser beams (one positioned on each side of the profile) having 6 kW, these beams were offset by 5 mm (this means one of the beams was ahead by 5 mm in relation to the second laser beam). A welding speed of 0.8 m/min and an entry angle of 10° was used to weld these profiles. Regarding the welded profiles, three 8 mm thick profiles and 25 mm thick profiles were produced, from each of the produced profiles three cross-sections were cut, resulting in 9 total samples per produced profile.

Due to the analyses that were to be carried out, special attention was given to sample preparation, especially due to the Electron Backscatter Diffraction (EBSD) analysis. Three cross-sections were obtained from each of the produced profiles (total of 6 produced profiles), for the thinner and thicker profile and were subsequently mounted in thermoset resin. The mounted samples were subject to grinding and polishing operations, firstly, these samples were ground using 4 sandpapers of differing grits, starting

with 200 grit, followed by 800, then 1000 and finally 1200 grit (for each grinding step the sample was rotated 90° in the same direction). Regarding the sample polishing, these were first subject to diamond polish, using two types of diamond slurry, on a first stage, a diamond polish with an average particle size of 3 μm, then another step, now using a 1 μm particle size diamond slurry, each of these steps lasts about 15 min. Finally, the mounted samples were polished using a colloidal Silica suspension, with a particle size of 50 nm, in this step, the samples were polished for 30 min.

Samples from both profile types were analyzed and their welds characterized, being subject to a microstructure analysis using Scanning Electron Microscopy (SEM) and EBSD, using a FEI Quanta 400FEG-SEM equipment (Field Electron and Ion Company, Hillsboro, OR, USA), provided with an EDAX Genesis X-ray spectroscope (EDS-energy dispersive spectroscopy).

The hardness (HV5) of the weld zones was also evaluated for both profiles, using a universal hardness testing equipment, according to the standard ISO 22826. After initial analysis, 1 cross-section from each produced profile was used for hardness testing, thus, a total of 3 samples per profile were tested, characterizing all the weld areas. The presented values were obtained from calculating the average hardness values and its standard deviation for each of the characterized weld zones.

3 Results and Discussion

Here, the results regarding the analysis of both laser-welded profiles are going to be presented. Showing the microstructure analysis and hardness characterization of the welds.

3.1 Thinner Profile Analysis – 8 mm

In Fig. 1, the cross-section of a welded 8 mm steel profile can be observed, the entry of the laser beam can be identified by the material reflux, producing as well, a “lack” of material at the exit of the laser beam (Fig. 1 b)). As can be observed, the profile was produced by a single pass, with the weld not presenting any defect.

The weld is divided into three distinct zones, the Fusion Zone (FZ), the Heat Affected Zone (HAZ) and the base material (BM), these were all identified in the SEM analysis, furthermore, EBSD analysis were carried out for this profile, being observed in Fig. 2. A grain refinement is observed in the HAZ, with the FZ presenting a coarse grain structure, due to the slow cooling of this zone. Hardness characterization of all these zones was carried out, with the mean values being presented in Fig. 3, the zone with highest hardness is the FZ, being followed by the HAZ and finally the BM.

3.2 Thicker Profile Analysis – 25 mm

As mentioned in Sect. 2, two laser beams were used for the welding of the thicker structural steel profiles. In Fig. 4 a), the macrostructure of the welded zone can be observed, with the identification of defects being also presented in Fig. 4 c) and d).

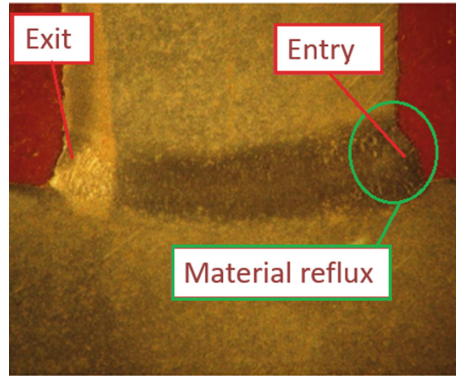


Fig. 1. a) Macrostructure of the produced 8 mm thick profile

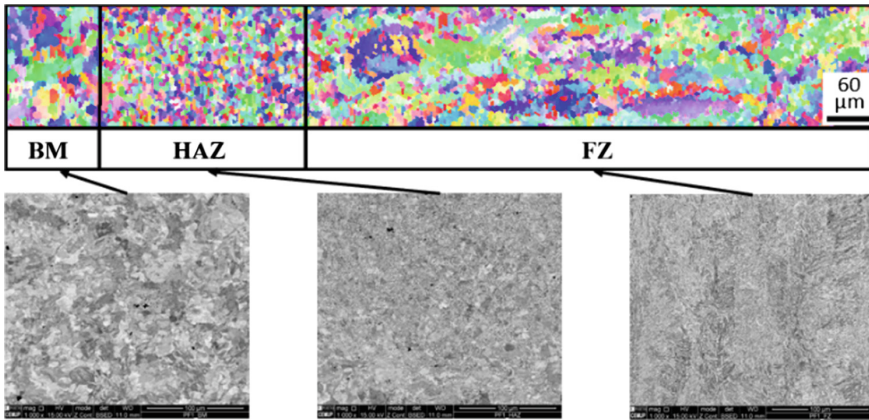


Fig. 2. Results of the EBSD analysis for each weld zone of the 8 mm thick profile

Analyzing Fig. 4, one of the weld beads is longer than the other, the longer one is the second pass, since the workpiece is already hot from the first pass the laser beam can achieve higher penetration. Despite using this strategy, defects were identified at the center of the weld. The two laser beams do not meet completely in the center, originating pores at the end of laser path (Fig. 4 b), possibly due to excessive laser power) and cracks due to lack of welding at the center of the weld bead. This can be observed in detail in Fig. 4 c), as there is no HAZ near the identified crack, it can be inferred that this defect originates from lack of heat in this area.

Regarding the EBSD characterization of the weld zones, the results obtained for the thicker profiles followed the same trend of those registered for the 8 mm thick profile, as seen in Fig. 5. There is a grain refinement in the HAZ, with the FZ presenting a coarser grain. However, the EBSD results are not as good as those obtained for the other profiles, this is since the thicker profile samples are harder to polish when compared to the thinner profiles, due to the bigger cross-section area.

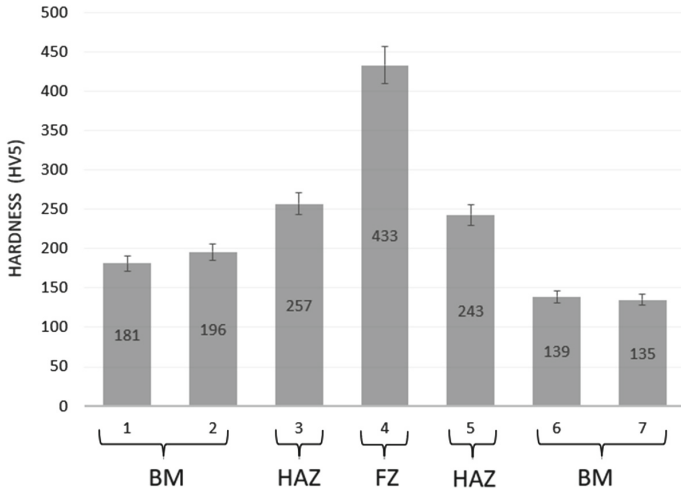


Fig. 3. Hardness values (HV5) for the weld zones of the 8 mm thick profile

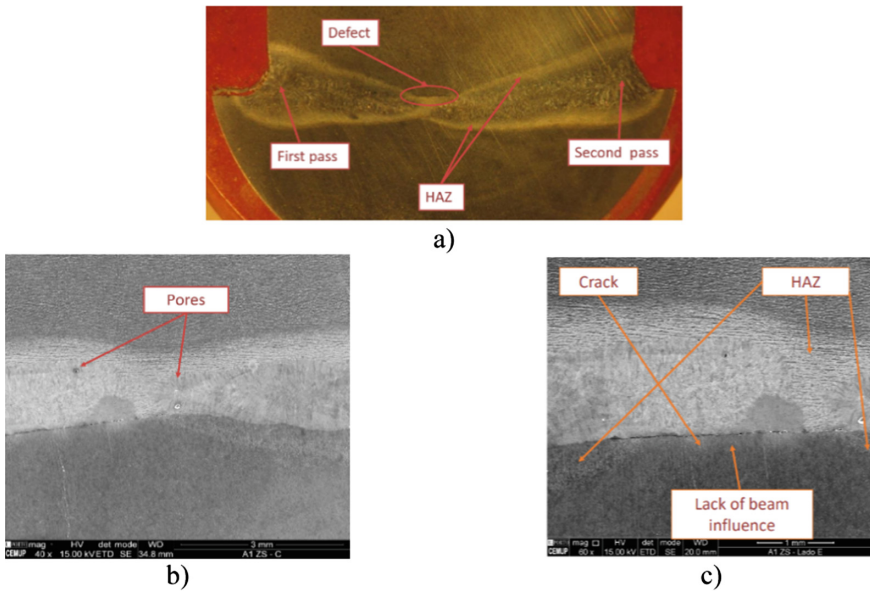


Fig. 4. a) Macrostructure of the 25 mm welded profile; SEM images of the weld center: b) Pore identification; c) Defect identification in the weld center

As for the hardness characterization of the welded zones of the 25 mm thick profiles, these were also very similar to those obtained for the thinner 8 mm profiles, these values can be observed in Fig. 6. Not only the values are quite similar, but the hardness variation is also the same, with the FZ presenting the highest hardness values, being followed by the HAZ and then finally the BM.

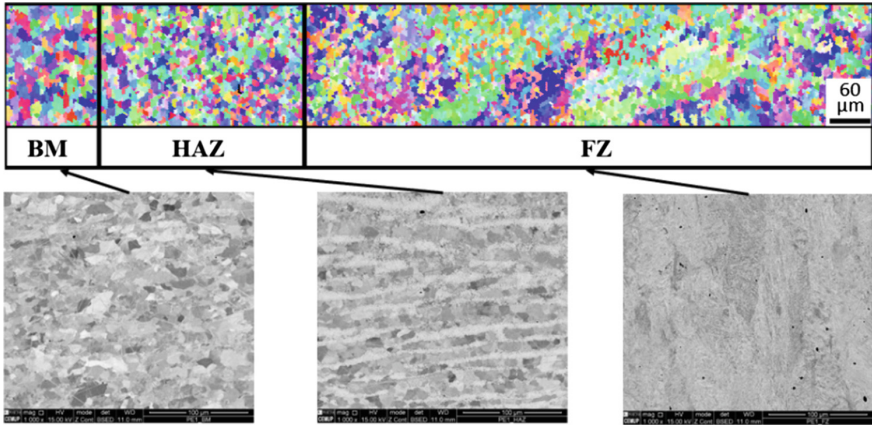


Fig. 5. Results of the EBSD analysis for each weld zone of the 25 mm thick profile

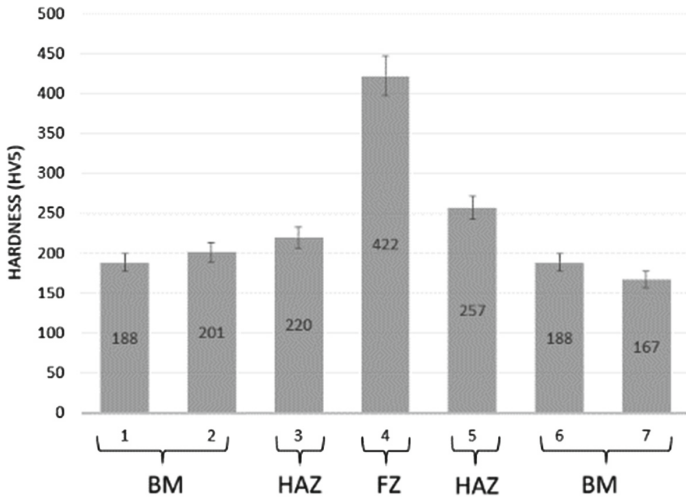


Fig. 6. Hardness values (HV5) for the weld zones of the 25 mm thick profile

4 Conclusion

In the present work, structural steel profiles were successfully produced by laser-welding. The following conclusions can be drawn:

- Quality welds were achieved for the 8 mm thickness S355JR steel profiles;
- A grain refinement in the HAZ was detected and confirmed by EBSD analyses;
- Hardness characterization was performed for all the weld zones, registering the highest hardness for the FZ, followed by the HAZ and, finally, by BM;
- Thick, 25 mm profiles, were successfully welded by using a double laser approach;

- The thick 25 mm profile welds presented the same behavior in terms of microstructure and hardness values as the 8 mm welded profiles, with a grain refinement being identified in the HAZ, and the FZ presenting a coarse grain. However, in terms of quality of EBSD analysis, the thicker profiles did not yield as good results as the thinner 8 mm thick profiles due to more difficult preparation of the samples.
- Weld defects were detected in the thicker welds, namely, pores and lack of welding;
- The pores were identified at the end of both laser beam paths, near the center of the thick profile welds. These originated due to excessive laser power;
- Regarding the crack, this was also identified at the center of the welded thick structural steel profiles, being caused by lack of heat supplied to this area;
- To correct the crack problem identified in these thick profiles, a more acute attack angle can be used, however, this may not be possible due to equipment/positioning restraints. Alternatively, the two laser beams could be positioned slightly higher, relative to the bottom steel plate, thus correcting this problem.

Despite the defects found in 25 mm-thickness profiles, these were welded successfully, with the possibility of correcting these problems by adjusting welding parameters and laser beam positioning. Furthermore, welding these structural steel profiles by this process brings many advantages, such as, a lower cycle time/production, especially when compared to the commonly employed process to produce these types of structural pieces. Additionally, the lack of filler metal reduces the weight of these profiles.

Acknowledgements. The authors thank to INEGI/LAETA and FLAD – Fundação Luso-Americana para o Desenvolvimento due to the support given to perform and present this work.

References

1. Sousa, V.F.C., Silva, F.J.G., Pinho, A.P., Pereira, A.B., Paiva, O.C.: Enhancing heat treatment conditions of joints in grade P91 steel: looking for more sustainable solutions. *Metals* **11**, 495 (2021). <https://doi.org/10.3390/met11030495>
2. Gouveia, R.M., et al.: Comparing the structure and mechanical properties of welds on ductile cast iron (700 MPa) under different heat treatment conditions. *Metals* **8**, 72 (2018). <https://doi.org/10.3390/met8010072>
3. Marques, E.S.V., Silva, F.J.G., Pereira, A.B.: Comparison of finite element methods in fusion welding processes—a review. *Metals* **10**, 75 (2020). <https://doi.org/10.3390/met10010075>
4. He, S., Liu, L., Zhao, Y., Kang, Y., Wang, F., Zhan, X.: Comparative investigation between fiber laser and disk laser: microstructure feature of 2219 aluminum alloy welded joint using different laser power and welding speed. *Opt. Laser Technol.* **141**, 107121 (2021). <https://doi.org/10.1016/j.optlastec.2021.107121>
5. Nilsen, M., Sikström, F., Christiansson, A.-K., Ancona, A.: In-process monitoring and control of robotized laser beam welding of closed square butt joints. *Procedia Manuf.* **25**, 511–516 (2018). <https://doi.org/10.1016/j.promfg.2018.06.123>
6. Grabmann, S., Tomcic, L., Zaeh, M.F.: Laser beam welding of copper foil stacks using a green high power disk laser. *Procedia CIRP* **94**, 582–586 (2020). <https://doi.org/10.1016/j.procir.2020.09.080>

7. Chen, N., Wan, Z., Wang, H.-C., Li, J., Yang, B., Solomon, J., Carlson, B.: Effect of ambient pressure on laser welding of AlSi10Mg fabricated by selected laser melting. *Mater. Des.* (2022). In press. <https://doi.org/10.1016/j.matdes.2022.110427>
8. Gonçalves, L.F.F.F., Duarte, F.M., Martins, C.I., Paiva, M.C.: Laser welding of thermoplastics: an overview on lasers, materials, processes and quality. *Infrared Phys. Technol.* **119**, 103931 (2021). <https://doi.org/10.1016/j.infrared.2021.103931>
9. Kolubaev, A.V., Sizova, O.V., Fortuna, S.V., Vorontsov, A.V., Ivanov, A.N., Kolubaev, E.A.: Weld structure of low-carbon structural steel formed by ultrasonic-assisted laser welding. *J. Constr. Steel Res.* **172**, 106190 (2020). <https://doi.org/10.1016/j.jcsr.2020.106190>
10. Luo, Z., Dai, J.S., Wang, C., Wang, F., Tian, Y., Zhao, M.: Predictive seam tracking with iteratively learned feedforward compensation for high-precision robotic laser welding. *J. Manuf. Syst.* **31**(1), 2–7 (2012). <https://doi.org/10.1016/j.jmsy.2011.03.005>
11. Grünenwald, S., Unta, A., Salminen, A.: Investigation of the influence of welding parameters on the weld geometry when welding structural steel with oscillated high-power laser beam. *Procedia CIRP* **74**, 461–465 (2018). <https://doi.org/10.1016/j.procir.2018.08.150>
12. Üstündağ, O., Gook, S., Gumenyuk, A., Rethmeier, M.: Mechanical properties of single-pass hybrid laser arc welded 25 mm thick-walled structures made of fine-grained structural steel. *Procedia Manuf.* **36**, 112–120 (2019). <https://doi.org/10.1016/j.promfg.2019.08.016>
13. Sokolov, M., Salminen, A., Kuznetsov, M., Tsibulskiy, I.: Laser welding and weld hardness analysis of thick section S355 structural steel. *Mater. Des.* **31**(10), 5127–5131 (2011). <https://doi.org/10.1016/j.matdes.2011.05.053>
14. Sokolov, M., Salminen, A., Somonov, V., Kaplan, A.F.H.: Laser welding of structural steels: Influence of the edge roughness level. *Opt. Laser Technol.* **44**(7), 2064–2071 (2012). <https://doi.org/10.1016/j.optlastec.2012.03.025>
15. Sokolov, M., Salminen, A., Katayama, S., Kawahito, Y.: Reduced pressure laser welding of thick section structural steel. *J. Mater. Process. Technol.* **219**, 278–285 (2015). <https://doi.org/10.1016/j.jmatprotec.2014.12.026>